Electronic Supplementary Material (ESI) for CrystEngComm.

SUPPLEMENTARY INFORMATIONS

A lanthanide functionalized MOF hybrid for ratiometric luminescent detection of an anthrax biomarker

Denan Zhang,[a] You Zhou,*[a] Jing Cuan,[b] Ning Gan

[a] Faculty of Materials Science and Chemical Engineering, Ningbo University, Ningbo 315211, Zhejiang, China. E-mail: zhouyou@nbu.edu.cn, ganning@nbu.edu.cn.

[b] Institute for Superconducting & Electronic Materials, School of Mechanical, Materials and Mechatronics Engineering, University of Wollongong, Wollongong, NSW 2522, Australia.

* Corresponding Author, E-mail: zhouyou@nbu.edu.cn

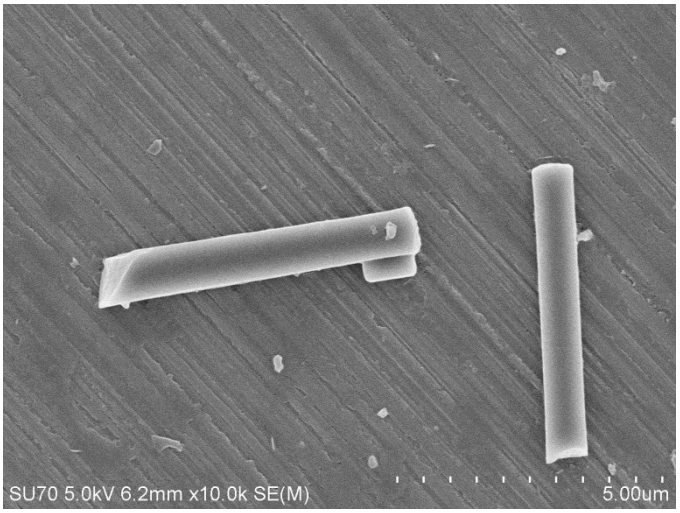

Figure S1. SEM images of Tb^{3+}@**1** microcrystalline rods.

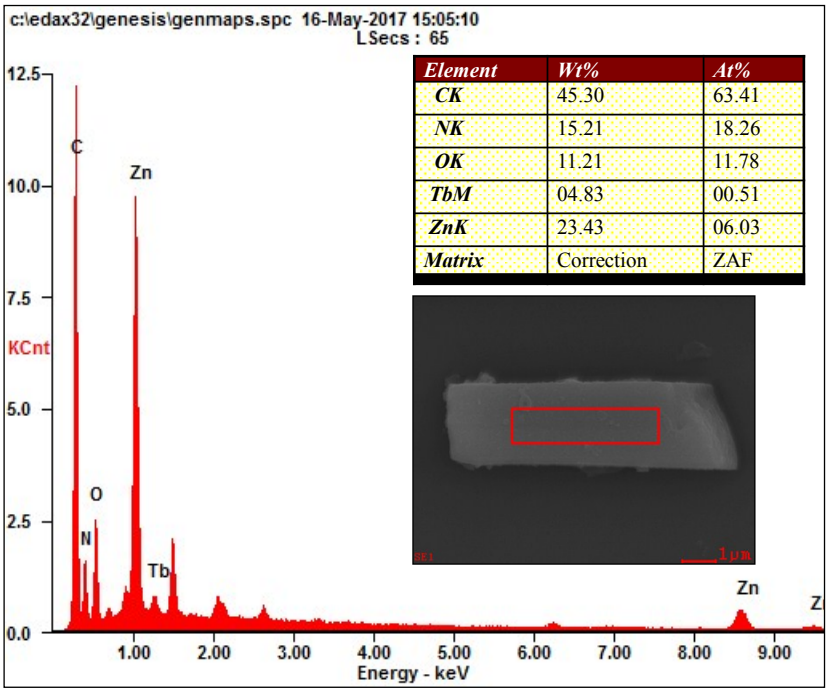

Figure S2. EDS spectrum of Tb^{3+}@**1**. The spectrum was recorded in the region marking with a red square on the microcrystal of Tb^{3+}@**1**, which is shown in the inset. The Table in the inset is results of mass ratios (Wt%) and atomic ratios (At%) of the elements.

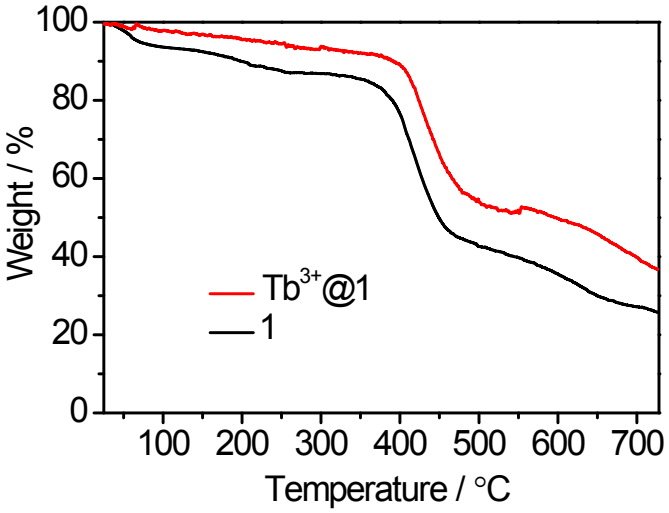

Figure S3. TGA curves of pristine 1 (black) and Tb^{3+}@**1** (red).

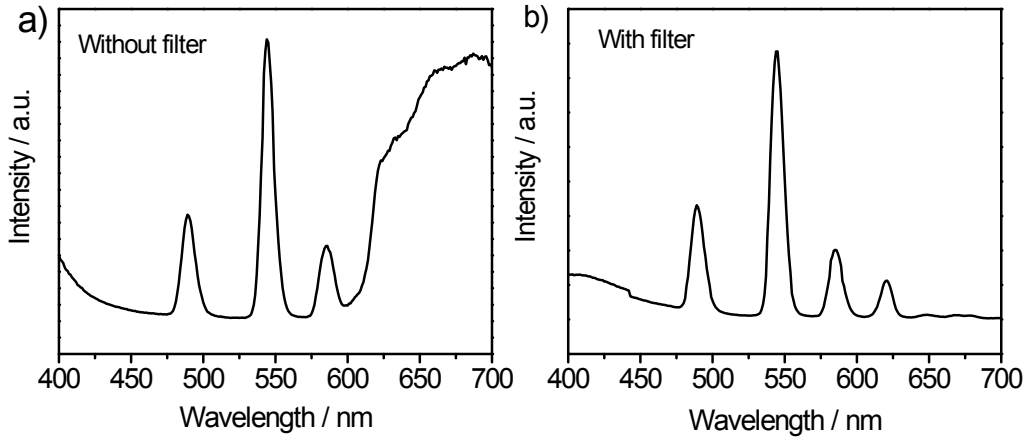

Figure S4. Emission spectra of Tb^{3+}@1 recorded without (a) and with (b) using a high-pass filter (400 nm). Both of the emission spectra are collected at the range of 400-700 nm.

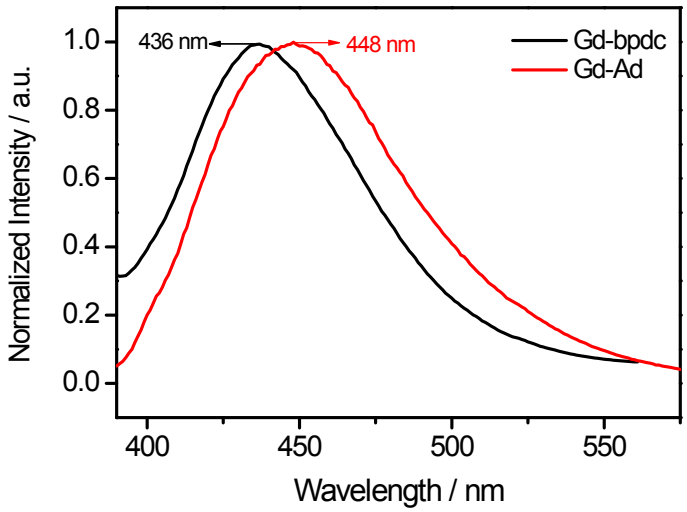

Figure S5. The phosphorescent spectra Gd-Ad (Ad, Adenine) and Gd-bpdc (bpdc, 4,4'-biphenyldicarboxylic) complexes recorded at 77 K.

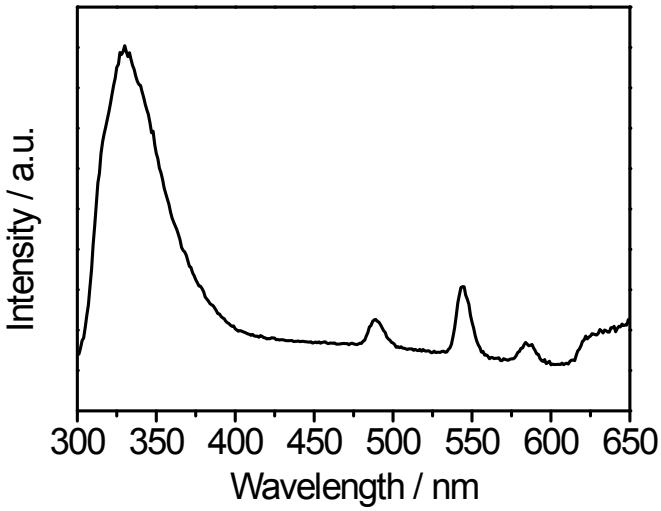

Figure S6. The photoluminescence emission spectrum of Tb^{3+}@**1** aqueous suspension.

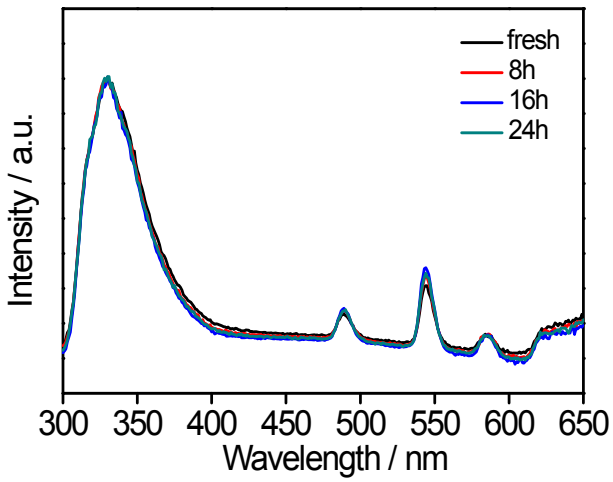

Figure S7. Time-dependent emission spectra of Tb^{3+}@**1** aqueous suspension.

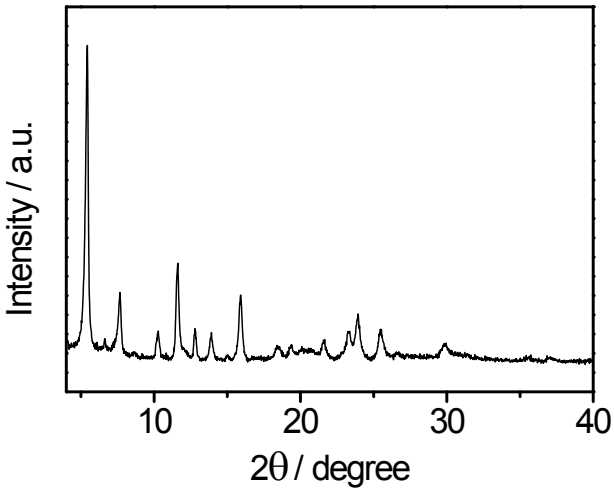

Figure S8. PXRD pattern of the Tb^{3+}@**1** sample after immersing in water for 24 h.

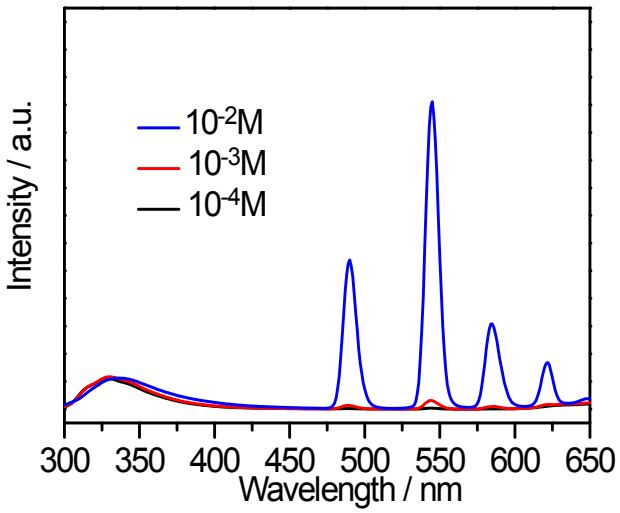

Figure S9. Emission spectra (λ_{ex} = 280 nm) of the Tb^{3+}@**1** products obtained with different feeding concentration (10^{-4}, 10^{-3}, 10^{-2} M) of $TbCl_3$.

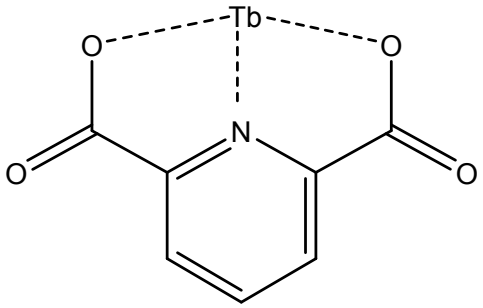

Figure S10. Schematic illustration of the chelation between DPA molecule and Tb^{3+}.

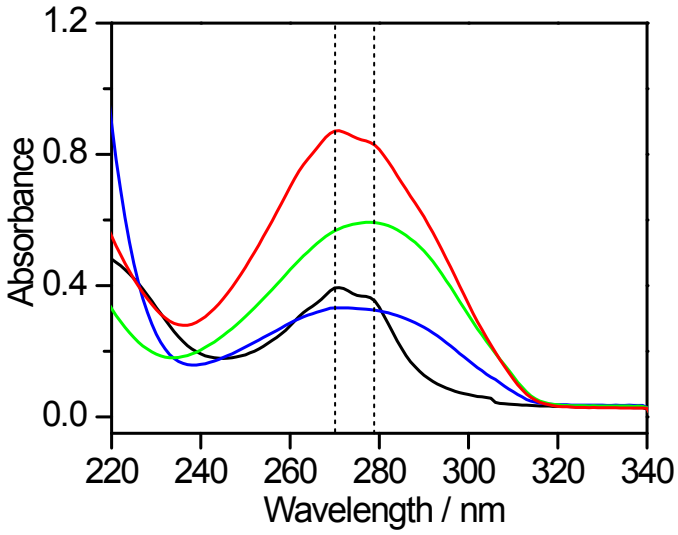

Figure S11. UV–vis spectra of DPA (black), pristine **1** (blue), Tb^{3+}@**1** (green) and the thoroughly washed Tb^{3+}@**1** (red) upon contacting with DPA.

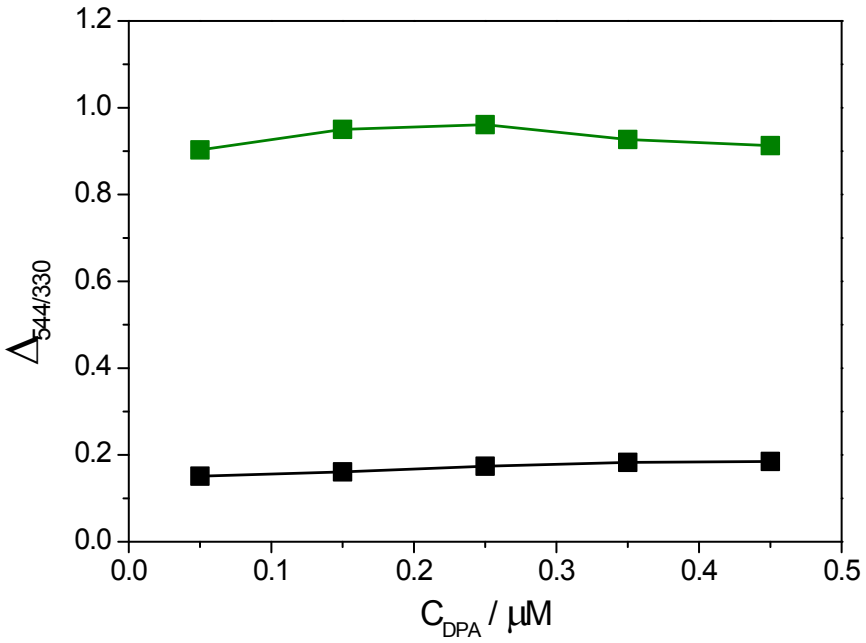

Figure S12. Emission intenisty ratios ($\Delta_{544/330}$) of various concentrations of Tb^{3+}@**1** in the presence (green) and absence (black) of DPA (1 μM).

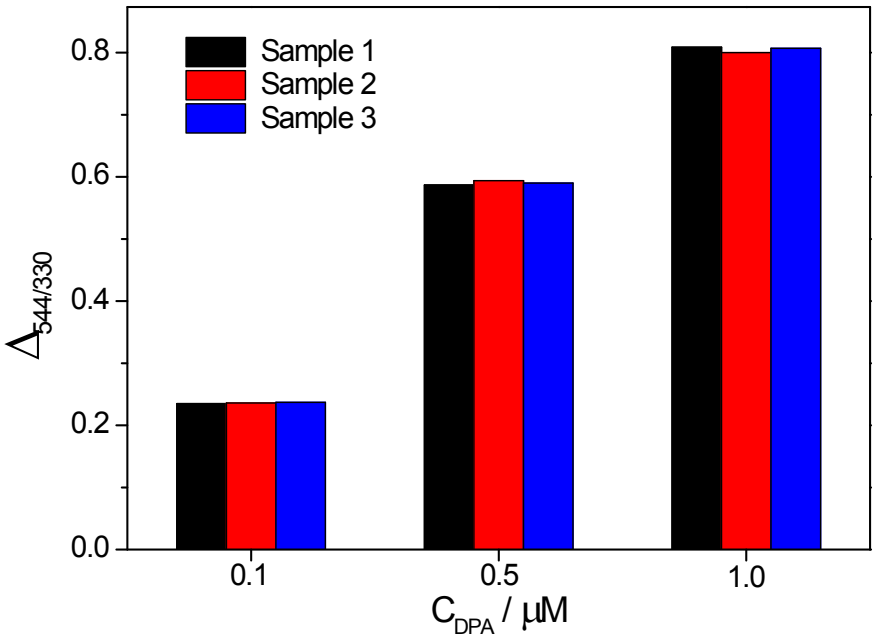

Figure S13. Emission intensity ratios ($\Delta_{544/330}$) of the Tb^{3+}@**1** prepared from different batches in different concentration of DPA.

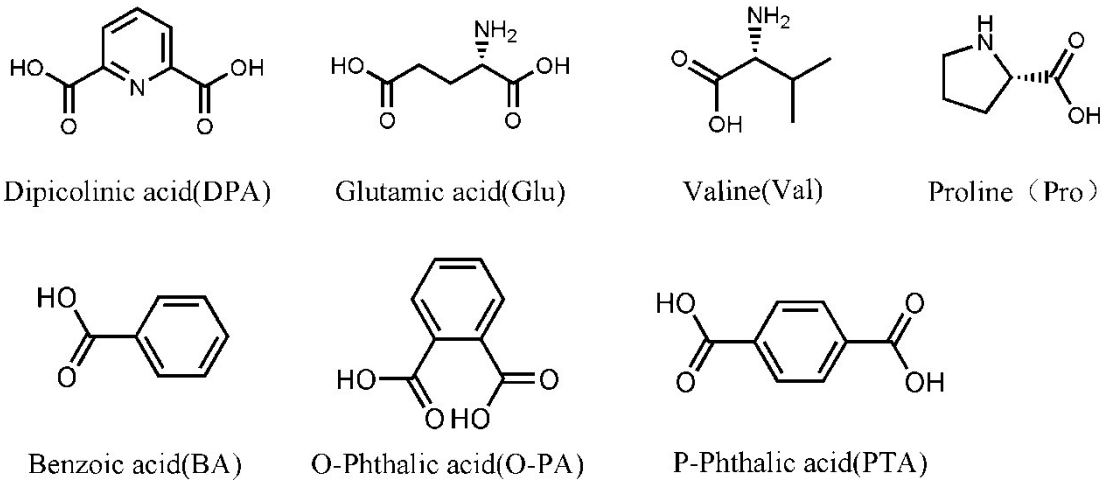

Figure S14. The molecular structures of DPA and interfering species used in this study.

Table S1. Detection of DPA in serum samples.

Added (nM)	Founded (nM)	Recovery (%)	RSD (n = 3) (%)
20	20.71 ± 0.26	103.55	1.25
100	109.4 ± 0.45	109.40	0.41
200	191.2 ± 0.35	95.60	0.18